

Chemical and Spectroscopic Characteristics of the Wood of *Vitis vinifera* Cv. Sangiovese Affected by Esca Disease

DIANA AGRELLI,[†] CARMINE AMALFITANO,^{*,†} PELLEGRINO CONTE,^{†,§} AND
 LAURA MUGNAI[‡]

[†]Dipartimento di Scienze del Suolo, della Pianta, dell'Ambiente e delle Produzioni Animali, Università degli Studi di Napoli Federico II, Via Università 100, Portici, Italy and [‡]Dipartimento di Biotecnologie Agrarie—Patologia Vegetale, Università degli Studi di Firenze, p.le delle Cascine 28, Firenze, Italy.

[§]Current address: Dipartimento di Ingegneria e Tecnologie Agro-Forestali (DITAF), Università degli Studi di Palermo, v.le delle Scienze 13, ed. 4, Palermo, Italy

Chemical and spectroscopic analyses (¹³C cross-polarization–magic angle spinning NMR and attenuated total reflection Fourier transform infrared spectroscopies) were carried out on the wood of *Vitis vinifera* cv. Sangiovese with brown-red discoloration and black streaks caused by esca disease. The analyses of the brown-red wood revealed the destruction of hemicelluloses and noncrystalline cellulose as well as modifications in the pectic and ligninic wood fractions. The pectic fraction consisted of carbohydrates associated with polyphenols. The lignin fraction exhibited only a few changes in the aromatic systems and a partial demethylation, and it appeared to be associated with condensed phenolic components probably arising from response polyphenols. The degradation of hemicelluloses and noncrystalline cellulose in brown-red wood, where the pathogens *Phaeoacremonium aleophilum* and *Phaeoconiella chlamydospora* prevail with respect to the other fungus *Fomitiporia mediterranea*, was consistent with reports on the degradative activity of such fungi in vitro carried out on model substrates. The observed alterations could also be attributed to the radical oxidation process caused by the oxidative response of defense itself triggered by infection, as suggested by the accumulation of postinfectious compounds. The analyses of wood tissue with black streaks showed less marked deterioration; here, an increase in pectic and phenolic substances, which probably accumulate in the xylem vessels as a response to the infection, was observed.

KEYWORDS: *Vitis vinifera*; esca disease; grapevine wood; ¹³C CP-MAS NMR

INTRODUCTION

Esca is a complex disease of grapevine trunk widespread all over the world (1), and it could be considered the result of interacting factors and numerous microorganisms acting together or a complex of five distinct syndromes among which is the so-called “esca proper” (2). Such a disease is often chronic and reduces grape harvest and quality (3). The characteristic leaf symptoms of infected plants appear in a discontinuous manner in time and space in the vineyard (1). The most evident symptoms in the trunks of vines affected simultaneously by vascular disease (young esca) and white rot, that is, esca proper (2), are black streaks (when seen in longitudinal trunk sections), various forms of discoloration from brown-red to black, and decaying white areas (1). The principal fungal pathogens involved in esca proper are *Phaeoconiella chlamydospora* (Pch) and *Phaeoacremonium aleophilum* (Pal), two ascomycetous fungi typically causing a vascular disease, and *Fomitiporia mediterranea* (Fmed), a basidiomycete causing white decay. The first two have been isolated

from tissue with brown-red discoloration or black streaks, while Fmed can be found mainly in decaying wood (1, 4).

Many studies on the enzymatic characteristics of these fungi and their ability to grow either on substrates containing different forms of carbon and nitrogen or on substrates enriched with various phenolic species have been carried out (1, 5–10) to understand how they attack wood tissues and colonize the host. However, studies focusing on the effects of Pch, Pal, and Fmed activity on the chemical modifications of wood tissue components have not yet been undertaken. Among other things, there are not so many chemical characterizations of the altered wood tissues from live plants attacked by rot fungi (11).

The aim of this study therefore was to examine the alterations in wood tissue with brown-red discoloration or black streaks in a grapevine plant affected by esca proper using chemical and spectroscopical techniques. This could be useful for better understanding of the colonization process of esca fungi, a quite slow one (12), which could further support a study aimed at esca control, unavailable at the moment.

MATERIALS AND METHODS

Chemical Analyses and Attenuated Total Reflection Fourier Transform–Infrared Spectroscopy (ATR-FTIR). The solvents for

*To whom correspondence should be addressed. Tel: 0039 0812539167. Fax: 0039 0812539186. E-mail: carmine.amalfitano@unina.it.

this study were acquired from Carlo Erba (Milan, Italy), and the deionized water was produced using the Milli-Q system (Millipore, Molsheim, France). Samples of brown-red wood (BRW) and asymptomatic wood (AW) were taken in Tuscany from cv. Sangiovese vines affected by esca disease. About 0.5 g of wood was cut into chips and powdered in liquid nitrogen as described earlier (13). From the same plants, samples of wood tissue (approximately 0.5 g) with black streaks (WBS) were carefully excised using a scalpel, freeze-dried, and ground in liquid nitrogen. The powdered woods were subjected to Soxhlet extraction with petroleum ether (100 mL for 8 h), and the wood residues were extracted in a 10 mL volume of methanol with agitation for 4 h in the dark and then extracted overnight with a further 10 mL of methanol with agitation. The residues were recovered by filtration through Whatman #41 filter paper (Maidstone, England) and then vacuum-dried. The remaining wood residues were subjected twice to a 12 h extraction with a 0.5% ammonium oxalate solution (50 mL) (Sigma-Aldrich, Milan, Italy) at 70–80 °C under reflux. The mixtures were then passed through Whatman #41 filter paper, and the residues were rinsed with hot water and vacuum-dried. The oxalate extracts together with the rinse waters were dialyzed in Spectra/Por tubes (Spectrum, Houston, TX) with a cutoff of 1000 Da. The dialyzed aqueous mixture from the BRW samples was extracted three times with approximately equal volumes of ethyl acetate. The dialyzed mixtures of oxalate extracts from the three woods (AW, WBS, and BRW) were freeze-dried to recover the pectic material. The rinsed wood residues were hydrolyzed to remove the hemicelluloses by boiling 100 mL of 0.05 M H₂SO₄ under reflux for 4 h. The hydrolyzed mixtures were then centrifuged to precipitate the wood residues, which were washed in water and vacuum-dried in a desiccator. The hydrolysis solutions were extracted with ethyl acetate, and the organic extracts were obtained by drying the ethyl acetate by rotary evaporation. The residues from the hydrolysis for hemicelluloses were hydrolyzed in 72% H₂SO₄ for 2 h with shaking to remove the cellulose, and the lignin residues were then recovered by filtration through a funnel with a sintered glass septum and washed and dried as described above for the other residues.

The wood residues obtained from the extraction and hydrolysis procedures were weighed, and the yields of extracts, hemicelluloses, and cellulose were determined by the weight losses of the residues, while the yields of pectic material and lignin residue were measured directly. FT-IR analysis by attenuated total reflection infrared spectroscopy was carried out using an FT-IR Spectrum One spectrometer (Perkin-Elmer, Waltham, MA) on the pectic substances and on the ethyl acetate extracts from the hydrolysis with 0.05 M H₂SO₄. The spectra obtained were transformed into transmission spectra and corrected for the baseline using the manufacturer's software (Spectrum v5.3.1, Perkin-Elmer).

Fenton Reaction. The Fenton reaction was carried out on a methanol extract obtained as described before from another sample of esca diseased wood from a Sangiovese grapevine that was also used to isolate the viniferins in a previous work (14). The methanol extract was dissolved in 1 L of water and then filtered on Whatman #41 filter paper. The concentration of the aqueous solution of methanol extract was determined on 5 mL of the solution by freeze drying and weighting the residue. The presence of stilbene metabolites was ascertained by high-performance liquid chromatography (HPLC) analysis as reported in a previous work (14). The solution was divided into three aliquots. One was used as a reference, whereas the remaining two were used to carry out the Fenton reaction with H₂O₂ and Fe²⁺. A solution of Fe²⁺ was prepared by dissolving 5 mmol of FeCl₂ × 4H₂O (Baker, Deventer, Holland) in 50 mL of water. The solution was filtered on a Whatman #41 filter paper and titrated in duplicate with a standard solution of K₂Cr₂O₇ (Carlo Erba) (Fe²⁺ = 0.0837 M, measured pH = 5), then diluted (8.37 mM), and stored in a He atmosphere at 4 °C. A solution (20.9 mM) of H₂O₂ was obtained by dilution of a commercial 35% H₂O₂ solution (AppliChem, Darmstadt, Germany). To one aliquot of the aqueous solution of the methanol extract under magnetic stirring, Fenton reactants were added as follows: First, a solution containing Fe²⁺ was added, followed immediately by a fresh H₂O₂ solution until molar ratios of 20 μmol/mg H₂O₂/Fe²⁺ and 3 μmol/mg H₂O₂/methanol extract were reached; the reaction was carried out for 24 h. To the other aliquot, the same amounts of Fe²⁺ and H₂O₂ were added; after, the H₂O₂ solution was repeatedly added to maintain a redox potential between 376 and 300 mV for 24 h. The reaction products and the methanol extract from control solution were recovered by freeze drying.

The freeze-dried materials were resuspended in the same initial volume of water and fractionated for their molecular mass using an Amicon cell (Beverly, MA) with a 10000 Da cut off.

¹³C Cross-Polarization–Magic Angle Spinning (CP-MAS) NMR Analyses. The wood samples and the residues obtained from each extraction and hydrolysis procedure were subjected to ¹³C CP-MAS NMR analysis. The spectra were acquired using a 300 MHz Bruker AVANCE NMR spectrometer (Bruker, Milan, Italy) equipped with a 4 mm Wide Bore MAS probe operating at 75.475 MHz on carbon-13. The sample was packed into a zircon rotor with a Kel-F cap and spun at 13000 ± 1 Hz. The instrument collected 1510 data points in an acquisition time of 20 ms with a recycling delay of 3 s. Each spectrum was accumulated with 2000 scans. For all of the spectra, a contact time of 1 ms was applied, while a RAMP sequence was used to account for the inhomogeneities of the Hartmann–Hahn condition at fast spin rates.

The spectra were processed using MestRe-C software (Version 4.9.9.9, Mestrelab Research, Santiago de Compostela, Spain). All of the free induction decays (FID) were transformed by applying a 4 K zero filling and an exponential filter function with a line broadening (LB) of 50 Hz. A multipoint baseline correction was done by using 14 points interpolated by a cubic function. No spinning side bands (SSB) were visible at the spinning rate used. For this reason, it was not necessary either to carry out a mathematical elaboration of the SSB or to apply a total suppression of side bands (TOSS) pulse sequence.

The spectra for the wood samples and their residues were divided and integrated into different resonance regions, with the natural peak valleys as limits. All of the regions were assigned to different molecular groups for the wood and their residues (with the exception of the lignin residue spectra) as follows (15, 16): 141–166 ppm, oxygenated aryl carbons, principally derived from C3 and C4 of the guaiacyl unit and C3 and C5 of the syringyl unit of lignin; 112–141 ppm, aryl protonated carbons or C substitutes, principally of lignin, and oxygenated C4 carbon of the syringyl unit of lignin; 94–112 ppm, mainly C1 acetal carbon from cellulose and aryl protonated carbons that are markedly shielded, such as C2 and C6 of the syringyl unit; 79–94 ppm, C4 carbons of polysaccharides, principally cellulose, and some alcoholic and ethereal sp³ carbons in the lignin side chains; 59–79 ppm, C2, C3, C5, and C6 of polysaccharides, principally cellulose, and some other alcoholic and ethereal sp³ carbons in the lignin side chains; 52–59 ppm, principally OCH₃ and some Cβ–C from lignin; and 0–52 ppm, total alkyl carbons, including the CH₃ in acetyl group (principally from hemicelluloses) at 21 ppm.

For the lignin residues, the intervals were subdivided as follows (15, 17, 18): 166–196 ppm, carboxylic carbon; 141–166 ppm, oxygenated aryl carbons, typically C4 from the *para*-hydroxyphenyl unit, C3 and C4 of guaiacyl, and C3 and C5 of syringyl; 97–141 ppm, protonated or C-substituted aryl carbons, including the oxygenated aryl C4 carbon of syringyl; 59–97 ppm, alcohol and ether sp³ carbons, principally Cα–O, Cβ–O, and Cγ–O from the lignin side chains; 52–59 ppm, OCH₃ and some Cβ–C from the lignin side chains; and 0–52 ppm, alkyl carbons, including other Cβ–C of the lignin side chains.

The amounts of the various carbons were expressed as percentages of spectrum area using the formula (RA/TA) × 100, where RA is the area of a particular spectroscopic region and TA is the total area of the spectrum. In addition, to assist in the comparison of different materials, same ratios of the areas (as percentages) of different spectroscopic regions were calculated. These percentages were considered affected by no more than 10% relative error as generally expected in such measurements (19).

The percentages of total carbohydrate carbons in the wood samples and their cellulose-containing residues were calculated as 6/5 of the spectroscopic area in the 59–94 ppm interval (polysaccharide carbons C2, C3, C4, C5, and C6) corrected by subtracting the contribution of the alcohol and ether sp³ carbons in the lignin side chains. This contribution was measured by determining the ratio between the areas of the spectrum for the intervals 59–94 and 112–166 ppm of the respective lignin residues and assuming that this ratio would remain the same in the spectra of the wood samples and their residues, since the 112–166 ppm signal for woods and their residues is mainly due to lignin.

The proportion of crystalline to amorphous cellulose was determined by taking the area of the C4 carbon signal at 89 and 84 ppm for the two forms of cellulose, respectively, and calculating the percentage ratio (20), corrected for the contribution of the carbons in the lignin side chains in

Table 1. Composition of Woods (% by Weight)

	AW	WBS	BRW
petroleum ether extract	0.7	0.8	0.5
methanol extract	5.6	6.7	6.9
oxalate extract	15.8	12.3	7.0
pectic substances	2.8	5.1	3.2
hemicelluloses	20.3	19.1	14.3
cellulose	45.4	43.8	41.4
cellulose/hemicelluloses	2.2	2.3	2.9
ligninic residue	12.1	17.2	29.9

that zone, as described above. The total aryl levels in the wood and its cellulose-containing residues were obtained by integrating the signal between 166 and 94 ppm, corrected for the contribution of the C1 carbohydrate carbons by subtracting 1/6 of the total carbohydrate carbons. It should be noted that because of limitations connected with ^{13}C CP-MAS NMR in the data quantification (15) and because of the arbitrary way used for spectra subdivision, the values obtained here are relative and can only be used for comparison of homogeneous materials, such as the wood samples in this study.

RESULTS AND DISCUSSION

Chemical Analyses. The results of the chemical analyses of the BRW, WBS, and AW samples are reported in **Table 1**.

Petroleum ether extracts were less than 1% for all samples. The methanol extracts were higher in the symptomatic woods, particularly BRW. Such methanol extracts have been ascertained to contain stilbene polyphenols, primarily resveratrol and ϵ -viniferin, typically produced by the *Vitis* genera in response to various types of stress and to accumulate in higher amounts in BRW (14, 21), as well as in WBS (unpublished data) in comparison to AW.

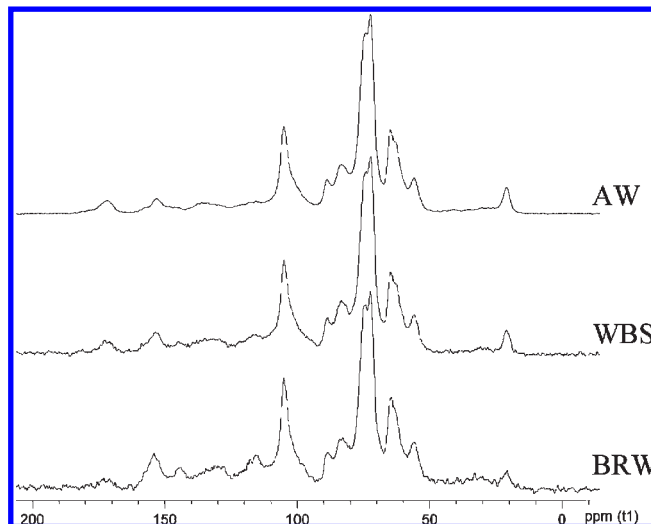
The oxalate extract was lower in BRW than in AW, while the pectic fraction showed an opposite trend. This suggests that BRW tissue contains lower amounts of low molecular weight water-soluble substances. Also, the oxalate extract from WBS was lower than AW but less markedly.

The water-pectin suspension from the BRW sample was brownish in color and remained brownish also after extraction with ethyl acetate that yielded only 4.4% organic extract. This was in contrast to the more usual whitish color of the analogues and total oxalate extracts from AW and WBS, and it suggested that this fraction was not constituted solely of pectins.

The largest pectic fraction was present in WBS. This and also the higher polyphenol content is attributable to the plant response to the infection, which takes the form of the accumulation of carbohydrate and polyphenolic substances in the xylem vessels with consequent occlusion (22); this may also extend to vessels that have not been directly invaded by fungal hyphae or that have not yet turned black. In fact, xylem injured function has been demonstrated to be also removed from the infection area (23), for example, eventual cavitations cause in any case a similar plant response (24). In these vessels, higher pectic levels could even favor the diffusion of Pch and Pal, if the polyphenols have not still formed a resistant barrier, given the ability of fungi to produce pectinolytic enzymes (7).

The cellulose and, even more markedly, the hemicellulose levels were lower in the diseased woods, particularly in BRW, as demonstrated by its higher cellulose/hemicelluloses ratios. The deterioration of hemicelluloses observed in BRW is consistent with the degradative action of Pch and Pal previously demonstrated in vitro (1, 5, 9). Diseased woods, in particular BRW, produced higher lignin residues. This is consistent with the low ligninolytic activity of Pch and Pal (1).

^{13}C CP-MAS NMR and ATR-FTIR Analyses. The ^{13}C CP-MAS NMR spectra for the woods and their containing cellulose

**Figure 1.** ^{13}C CP-MAS NMR spectra of AW, WBS, and BRW.

residues showed similar profiles but with slight differences in the intensity of the signals. In all of the spectra (**Figure 1**), the polysaccharide carbon signal (attributable to cellulose, hemicelluloses, and pectin) predominated in the 59–112 ppm interval, overlapping with the signals from various protonated aromatic carbons due to lignin in the 94–112 ppm interval, and etheral and alcoholic sp^3 carbons from the side chains of lignin in the 59–94 ppm interval. The signal between 196 and 166 ppm was due to the carbons of the COO(H,R) group, primarily acetyl group of the hemicelluloses, although their levels may be underestimated due to the known low instrumental sensitivity for quaternary carbons (15). The signals in the 112–166 ppm interval arose from the oxygenated, C-substituted, or protonated aromatic carbons of lignin. The signal at 56 ppm was mainly due to the OCH₃ and C β -C of lignin, while the signal at 21 ppm was due to the acetyl CH₃ of hemicelluloses.

The ^{13}C CP-MAS NMR quantitative data for the wood samples and their residues after each extraction and the hydrolysis of hemicelluloses are shown in **Table 2**. The levels of total aryl carbons, their aryl-O(H,R) and aryl-(H,R) fractions, and the C_{sp³}-O(H,R) of the lignin side chains were generally higher in the diseased woods, especially BRW. Total carbohydrate carbons showed an opposite trend, markedly for BRW, less evident for WBS. The 56 ppm signal did not markedly diminish following the extraction and hydrolysis steps, confirming that this signal is essentially derived from the OCH₃ and C β -C of lignin.

The percentages of the various types of carbons for all of the wood residues after petroleum ether extraction did not show evident differences from those for the original wood tissues. Conversely, after methanol extraction, the percentages of total carbohydrate carbon increased due to the decrease of the total aryl carbons, confirming that extraction of the polyphenols had occurred. The higher decrease in the percentage of COO(H,R) after methanol extraction in AW and WBS suggested the presence of higher levels of extractable carboxylic species in these tissues than in BRW.

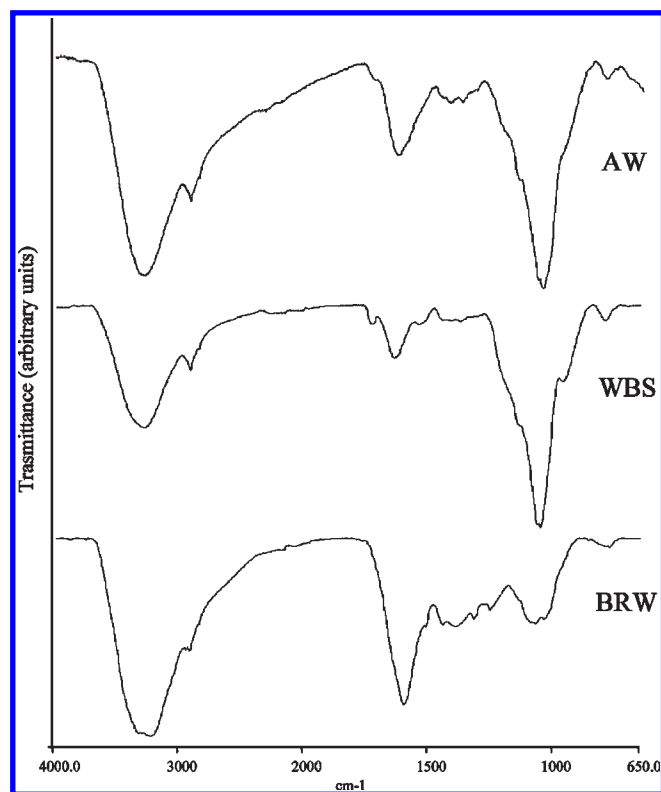
After oxalate extraction, a decreasing trend in total carbohydrate carbons was found in the AW residue, and even more so in the WBS residue, as compared to the residues after methanol extraction, which agrees with the pectin levels recorded in the chemical analyses (**Table 1**). The increase in COO(H,R) observed for AW and WBS could be due to residues of oxalate in the samples. In BRW after oxalate extraction, the carbohydrate

Table 2. Percentages of the Structural Carbon by ^{13}C CP-MAS NMR of Woods and Their Residues Obtained after Extraction and Hydrolysis Treatments

treatments	woods	-COO- (H,R)	aryl-O- (H,R)	aryl- (H,R)	aryl (total)	C _{sp3} -O- (H,R)	carbo- hydrates	cryst./ amorph. cellulose	OCH ₃ + Cβ-C	total alkyls	acetyl CH ₃
none	AW	2.6	4.0	11.7	15.7	6.5	65.1	50.0	4.6	5.5	3.2
	WBS	2.6	5.9	16.0	21.9	8.6	58.3	47.8	4.6	4.0	2.4
	BRW	1.4	9.1	21.9	31.0	10.3	48.3	48.5	4.8	4.1	1.6
petroleum ether extraction	AW	2.7	4.2	11.9	16.1	6.5	64.0	50.7	4.6	6.1	3.1
	WBS	2.3	5.4	15.6	21.0	8.1	59.6	50.7	4.3	4.6	2.1
	BRW	1.8	9.0	22.0	31.0	10.0	48.5	46.6	4.3	4.4	1.8
methanolic extraction	AW	1.6	2.8	8.6	11.4	4.5	72.3	46.1	5.4	4.9	3.2
	WBS	1.4	3.5	11.1	14.6	5.4	70.7	49.4	5.0	2.8	2.4
	BRW	1.4	6.9	17.9	24.9	8.0	58.5	48.6	4.4	2.8	1.5
ammonium oxalate extraction	AW	2.1	3.4	10.4	13.9	5.4	71.1	47.4	4.6	2.9	2.4
	WBS	2.1	4.4	11.6	15.9	6.1	66.7	50.7	5.1	4.1	2.1
	BRW	1.3	4.9	15.5	20.4	6.5	59.9	54.0	5.2	6.7	2.0
hydrolysis with 0,05 M H ₂ SO ₄	AW	2.2	4.1	12.2	16.3	6.8	64.2	59.9	5.9	4.6	1.4
	WBS	1.2	4.4	15.1	19.5	7.4	63.1	71.8	5.1	3.7	1.7
	BRW	1.5	6.8	20.8	27.6	9.0	52.7	67.2	4.5	4.7	1.5

carbon levels tended to increase, concurrently the aromaticity decreased, in contrast to what was observed for AW and WBS. This could be due to the fact that the extracted pectic substances were accompanied by aromatic structures, which could have imparted to the pectins the brownish color observed. In fact, while the ATR-FTIR spectra of the pectic substances from AW and WBS showed only the expected signals (peaks or shoulders at 1148, 1072, and $\approx 1050\text{ cm}^{-1}$ from C-O of the secondary alcohols; 962 cm^{-1} from the methylene group; and 1728 cm^{-1} from the carboxylic group), the ATR-FTIR spectra of the pectic substances from BRW also showed phenolic signals (1603 , 1514 , and 1446 cm^{-1} from the aromatic rings and 1383 and 1259 cm^{-1} from OH and C-O in the phenoxy groups, respectively) together with other signals typical for carbohydrates, also after extraction with ethyl acetate (Figure 2) (25). This would suggest that the pectic fraction from BRW consists of carbohydrate and phenolic structures. It is possible that this fraction is predominantly made up of polysaccharide fragments derived from wall structures, linked to lignin residues or response polyphenols, rather than of pectic residues; in fact, the IR band of the carboxylic groups typical of pectins was not present (Figure 2).

In all of the wood samples, the levels of carbohydrate carbon generally reduced after 0.05 M H₂SO₄ hydrolysis due to the splitting off of hemicelluloses (Table 2). Hemicelluloses removal was confirmed by the decrease in acetyl carbons, although the small remaining amounts of the latter suggest that the hemicelluloses were not totally eliminated. The ATR-FTIR spectra (Figure 3) of the ethyl acetate extracts of the 0.05 M H₂SO₄ hydrolysis solutions from AW and WBS (about 1% wood each) showed signals at 1739 and 1716 cm^{-1} attributable to ester linkages; 1612 and 1514 cm^{-1} associated with the aromatic rings; 1216 cm^{-1} due to the C-O of phenoxy groups; 1117 and 1049 cm^{-1} attributable to alcoholic C-OH; and 1264 and 1034 cm^{-1} arising from OCH₃ (26). These signals can be attributed to feruloyl carbohydrates deriving from ferulic acid esterification with hemicelluloses (27). However, the ATR-FTIR spectrum of the analogue extract from BRW (1% wood), although quite similar to those from AW and WBS, presented less marked methoxyl bands, suggesting that the feruloyl underwent demethylation. Furthermore, this spectrum exhibited more intense bands at 1216 and 1612 cm^{-1} , as well as the appearance of a band at 1706 cm^{-1} , probably indicating aryl carboxyl groups; this points to the presence of further oxy-benzoic acids, which could also

**Figure 2.** ATR-FTIR spectra of pectic substances extracted from AW, WBS, and BRW after ethyl acetate extraction.

arise from the degradation of feruloyl carbohydrates, beginning with their hydrolysis and the successive destruction of the vinyl group. This could be coherent with the tannase activity of Pch and Pal demonstrated toward gallotannins in *in vitro* experiments (8).

The percent ratio of C4 signal of crystalline (89 ppm) and noncrystalline (84 ppm) carbohydrate carbon (crystalline/amorphous) showed no evident differences among the three kind of woods and their residue until methanol extraction (Table 2). After ammonium oxalate extraction, an increasing trend was observed only for BRW. This could be due to a split off of some sp³ oxygenated carbons associated with wood polyphenolic components such as in lignin fragments and condensed viniferins contributing to the signal at 84 ppm rather than only a depletion of

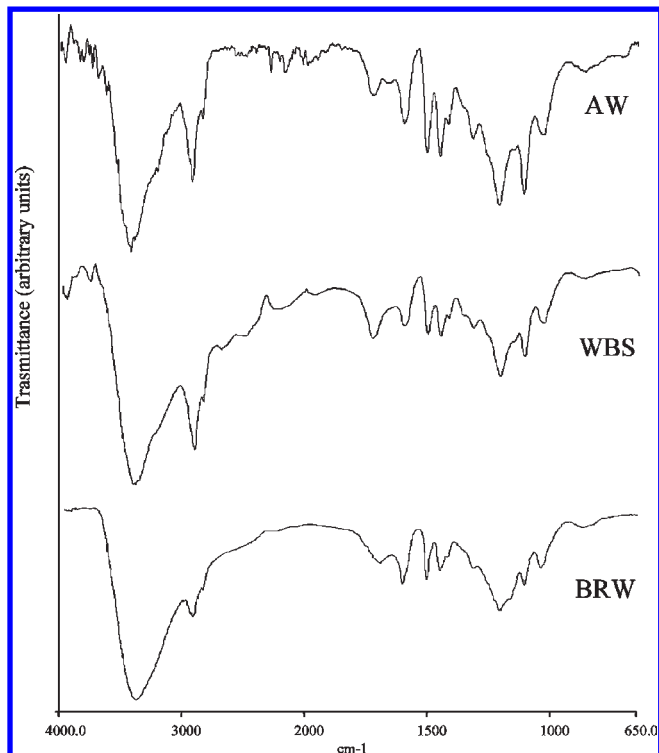


Figure 3. ATR-FTIR spectra of the ethyl acetate extracts of 0.05 M H₂SO₄ hydrolysis solutions of AW, WBS, and BRW.

noncrystalline C4 from soluble fragments of partially degraded structural carbohydrates.

After the hydrolysis for hemicelluloses, a marked increase in crystalline cellulose in comparison to amorphous cellulose was evident (**Table 2**). These percentages were higher for BRW and WBS than AW, suggesting that in these residues, in addition to hemicelluloses, a fraction of noncrystalline cellulose was depleted probably because it was decomposed as a consequence of *esca* fungi attack. In addition, the fact that the alteration primarily involved the noncrystalline (rather than the crystalline) cellulose is in agreement with the demonstrated enzymatic activity of the endoglucanase, but not the exoglucanase, of Pch and Pal (*1, 28*).

All of the spectra for the lignin residues (**Figure 4**) showed typical lignin signals (*15, 29*) attributable to oxygenated aromatic carbons between 141 and 166 ppm; C4–O of syringyl, protonated aromatic, and C-substituted carbons between 97 and 141 ppm; lignin side chain carbons C α –O, C β –O, and C γ –O between 59 and 97 ppm, in particular C γ –OH at 60 ppm; methoxyl carbons and a portion of the C β –C from the side chains at 56 ppm; and alkyl carbons and other C β –C from the side chains between 0 and 52 ppm. A weak carboxyl carbon signal was also observed at 174 ppm.

In the spectra of the lignin residue for AW (**Figure 4**), the signal at 153 ppm was markedly less intense than the remaining resonances of aryl–O. In the angiosperm lignin, this signal is mainly due to C3 and C5 of syringyl units etherified at C4 (resonating at about 135 ppm) and C4 of *p*-hydroxyphenyl (*15, 29*). Thus, in the grapevine lignin, only small amounts of *p*-hydroxyphenyl and/or etherified syringyl units were probably present. At the same time, the higher signal at 108 ppm attributable to C2 and C6 (*15*) in syringyl structures, typical for angiosperm lignin, than that at 115 ppm due to C2, C5, and C6 in guaiacyl, typical for gymnosperm lignin in which only guaiacyl is present, suggested a prevailing presence of syringyl. Thus, no etherified syringyl at C4 should be present in grapevine lignin. Unfortunately, it was not possible to determine the relative

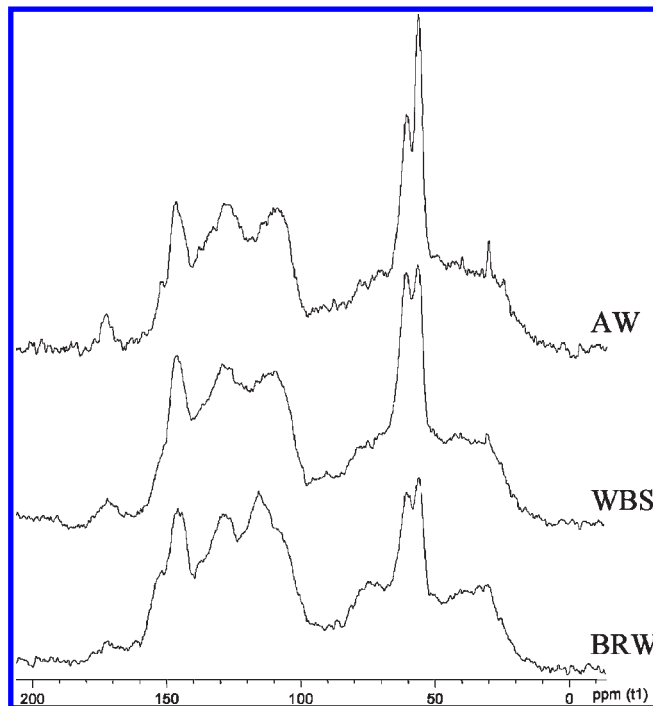


Figure 4. ¹³C CP-MAS NMR spectra of the lignin residues of AW, WBS, and BRW.

amounts of guaiacyl, having one methoxyl group, with respect to syringyl, with two methoxyl groups, by the levels of methoxyl signal in comparison to those of total aromatic carbons or aryl–O. This is because aromatic quaternary carbon response to ¹³C CP-MAS NMR may be less sensitive than that of methoxyl (*15*) and the methoxyl signal probably overlaps the signal of some C β –C and other aliphatic carbons. However, other authors have evidenced by hydrolytic demolition methods the presence of structural units mainly related to guaiacyl and *p*-hydroxyphenyl, together with a low amount of methoxyl group, in grapevine woods (*30*). About *p*-hydroxyphenyl, it could be scarce in lignin isolated by hydrolysis as that examined here because such an unit could be depleted because it is bounded by hydrolyzable ester linkages in woods. The prevalence of guaiacyl rather than syringyl implies an alternative attribution of the signal around 108 ppm. Such a signal could be due to carbons in guaiacyl units, which are primarily condensed on C5. In this case, the three guaiacyl carbon signals at about 115 ppm move out of their location: C2 toward about 108 ppm, C5 toward higher shift, and C6 toward both higher or lower shift (also close to 108 ppm) depending on the kind of substitution to C5 (*18*).

The higher intensity of the signal at about 60 ppm in the lignin residue for AW (**Figure 4**) indicates that in grapevine lignin C γ is not involved in the condensation of the monomeric units; for example, the structural unit such as pinoresinol, for which C γ resonates at 72 ppm, is barely present (*17*). The lignin from WBS (**Figure 4**) showed essentially the same characteristics as the lignin from AW in terms of aromaticity, but the signal intensity of methoxyl was lower (**Table 3**).

The ¹³C CP-MAS NMR spectrum of the lignin residue from BRW (**Figure 4**) showed higher total aromatic carbons than the spectrum for AW (**Table 3**). Furthermore, typical signs of the destruction of aromaticity produced by fungal activity such as white rot fungi, for example, the cleavage of aromatic rings via the 3-oxoadipate oxidative pathway, leaving behind alkyl ketoacid residues (*31*), were not evident. In fact, ketone signals around 200 ppm were absent, and a decrease in total alkyl was noted,

Table 3. Percentages of the Structural Carbon of Lignin Residues from AW, WBS, and BRW by ^{13}C CP-MAS NMR

	-COOH	aryl-O(H,R)	aryl-(H,R)			aryl (total)	aryl-O/aryl	$\text{C}_{\text{sp}^3}\text{-O(H,R)}$	$\text{OCH}_3 + \text{C}\beta\text{-C}$	alkyl + $\text{C}\beta\text{-C}$
			141–118 ppm	118–97 ppm	total					
AW	1.5	11.2	19.3	16.0	35.3	46.5	24.1	21.2	11.2	19.6
WBS	1.3	12.1	19.9	16.9	36.9	49.0	24.8	21.7	9.9	18.0
BRW	1.7	15.1	20.7	19.1	39.7	54.9	27.6	20.1	7.9	15.3

although the carboxylic acidity was slightly increased. The higher aromaticity of the lignin residue from BRW was primarily due to the increase of 115 ppm signal and of aryl-O resonance, the latter is also confirmed by the higher aryl-O/aryl percentage. Furthermore, a widening of the aryl-O signal toward higher shifts was evident (**Figure 4**).

Essentially, the lignin residues of WBS and BRW did not show variation of $\text{C}_{\text{sp}^3}\text{-O}$ signal (**Table 3**) suggesting no evident oxidative decay of side chain structures, as proved also by no evident increase of any carboxyl (31). Thus, also the other $\text{C}\beta$ resonating at lower shift ($\text{C}\beta\text{-C}$) very probably remained unaltered as well as their contribution to the 56 ppm signal. Consequently, the 56 ppm signal reduction recorded in WBS and even more in BRW lignin residues (**Table 3**) could be essentially attributed to a depletion of methoxyl groups of the lignins of these woods as evidenced in demethylation processes caused by microorganisms (31). There was in lignin residue from diseased woods also a reduction in alkyl carbon content, particularly for BRW lignin residue (**Table 3**), that did not probably depend on degradation of side chain carbons for the reasons above-mentioned. Neither demethylation of lignin units, nor the hydroxylation of guaiacyl and *p*-hydroxyphenyl, nor an eventual modification of the side chains, all typical degradation processes of lignin (31), would have caused shifts in the protonated aromatic carbon resonances sufficient to increase the 115 ppm signal to the levels observed in BRW lignin residue. This suggests that there was a further addition in polyphenols causing such signal increase.

In the ^{13}C CP-MAS NMR spectra of the polyphenol condensation products obtained after subjecting the methanol extracts of diseased wood [extracts containing stilbene polyphenols (viniferins) (14) and probably also glycosylate polyphenols, which could also be ligninic in nature] to the Fenton reaction, the signal at 115 ppm tended to prevail and the signal at 145 ppm to increase as condensation proceeded (**Figure 5**). Furthermore, the low field signal at 155 ppm denoting the phenolic carbons of the viniferins remained evident (14, 21). The increases in the 115 and 145 ppm signals could be due to the formation of condensed viniferins by aromatic ether linkages involving their *p*-hydroxyphenyl units in the *ortho* position to the hydroxylate carbon. In addition, the signals of the nonoxygenated carbons of the 3,5-dihydroxy-substituted rings (typical in viniferins), resonating around 100 ppm, evident in methanol extract spectrum, tend to diminish in reaction product spectra probably because these carbons were involved in condensation that shift their resonance toward higher values. All of the mentioned signals of such products from the Fenton reaction corresponded with those that increased in the spectra of the BRW lignin residue, suggesting the contribution of such condensed species to the aromaticity of BRW.

The observed alteration of lignin aromaticity in BRW suggests low ligninolytic activity of Pch and Pal, although *in vitro* these fungi occasionally exhibit polyphenoloxidase and peroxidase activity (1, 5, 9) and the ability to grow on substrates enriched with various polyphenols (6, 8). The inability of Pch and Pal to cleave aromatic rings could be due to the availability of carbohydrates. For example, *in vitro* assays have shown that the decomposition of lignin polymers by the fungi of brown rot decreases as

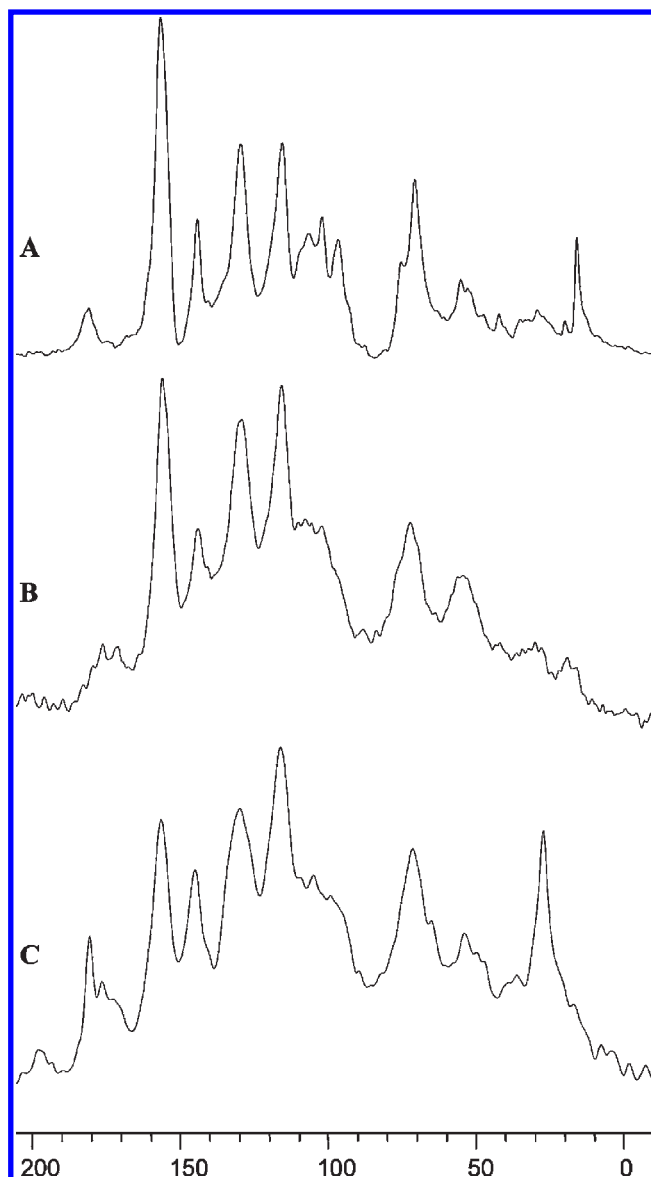


Figure 5. ^{13}C CP-MAS NMR spectra of methanol extract from diseased wood subjected to Fenton reaction. (A) Control, (B) after 24 h of reaction, and (C) repeated additions of H_2O_2 maintaining redox potential between 376 and 300 mV for 24 h. The products B, C, and A yielded 17, 33, and <1% molecular mass fractions >10000 Da, respectively.

carbohydrate availability increases (31). However, the lignin may have been protected from the attack of Pch and Pal, and probably also Fmed, a ligninolytic fungus that usually is not abundant in BRW (1), by the formation of aromatic ethers through condensation with the response polyphenols that appear to have contributed (in their condensed form) to the lignin fraction of the BRW. This could have blocked the transformation of ligninic structures into catechol-like species, the precondition for the demolition of lignin aromaticity (31).

In BRW, the alterations observed may also be attributed to radical oxidation, which could have led to the demethylation of

lignin (32) and the formation of the condensed polyphenols associated with lignin and carbohydrates in the pectic fraction, the latter of which probably contains degraded pectins and fragments of hemicelluloses and cellulose. Similar alterations are produced during the decay caused by the fungal agents of brown rot, which induce the production of H₂O₂ and complex iron, triggering a Fenton-like reaction that predisposes the wood tissue to enzyme attack on its carbohydrate fraction and leads to slight alterations in the lignin (32, 33). In the case of BRW, this process could be caused by the oxidative defense response itself, as evidenced by the accumulation of large amounts of polyphenols implicated in disease defense (14, 34).

ACKNOWLEDGMENT

We thank Prof. Alessandro Piccolo [chief of Centro di Ricerca Interdipartimentale sulla Risonanza Magnetica Nucleare (NMR) per l'Ambiente, l'Agro-Alimentare ed i Nuovi Materiali, CER-MANU, Portici, Italy] for the NMR facilities and suggestions and Professors Antonio Evidente (Dept. Scienze del Suolo, della Pianta, dell'Ambiente e delle Produzioni Animali, Portici, Italy) and Giuseppe Surico (Dept. Biotecnologie Agrarie—Patologia Vegetale, Firenze, Italy) for suggestions.

LITERATURE CITED

- Mugnai, L.; Graniti, A.; Surico, G. Esca (black measles) and brown wood-streaking: Two old and elusive diseases of grapevines. *Plant Dis.* **1999**, *83*, 404–417.
- Surico, G. Towards a redefinition of the diseases within the esca complex of grapevine. *Phytopathol. Mediterr.* **2009**, *48*, 5–10.
- Calzarano, F.; Seghetti, L.; Del Carlo, M.; Cichelli, A. Effect of esca on quality of berries, musts and wines. *Phytopathol. Mediterr.* **2004**, *43*, 125–135.
- Fischer, M.; Kassemeyer, H. H. *Fomitiporia mediterranea*, a new basidiomycete species associated with esca of grapevine in Europe: Biology, ecology, and distribution. *Phytopathol. Mediterr.* **2004**, *43*, 144.
- Mugnai, L.; Surico, G.; Sfalanga, A. Produzione di enzimi esocellulari da parte di funghi del legno di viti colpite dal "mal dell'esca". *Micologia Ital.* **1997**, *1*, 11–22.
- Mugnai, L.; Bertelli, E.; Surico, G.; Bruno, E. Effetto di alcune sostanze fenoliche sulla crescita di funghi del legno di viti colpite dal "mal dell'esca". *Petra* **1997**, *11*, 35–46.
- Marchi, G.; Roberti, S.; D'Ovidio, R.; Mugnai, L.; Surico, G. Pectic enzymes production by *Phaeoconiella chlamydospora*. *Phytopathol. Mediterr.* **2001**, *40*, S407–S416.
- Bruno, G.; Sparapano, L. Effect of three esca-associated fungi on *Vitis vinifera* L.: III. Enzymes produced by the pathogens and their role in fungus-to-plant or in fungus-to-fungus interactions. *Physiol. Mol. Plant Pathol.* **2006**, *69*, 182–194.
- Santos, C.; Fragoeiro, S.; Valentim, H.; Phillips, A. Phenotypic characterisation of *Phaeoacremonium* and *Phaeoconiella* strains isolated from grapevines: enzyme production and virulence of extracellular filtrate on grapevine calluses. *Sci. Hortic.* **2006**, *107*, 123–130.
- Mazzullo, A.; Di Marco, S.; Osti, F.; Cesari, A. Bioassays on the activity of resveratrol, pterostilbene and phosphorus acid towards fungi associated with esca of grapevine. *Phytopathol. Mediterr.* **2000**, *39*, 357–365.
- Rolshausen, P. E.; Greve, L. C.; Labavitch, J. M.; Mahoney, N. E.; Molyneux, R. J.; Gubler, W. D. Pathogenesis of *Eutypa lata* in grapevine: Identification of virulence factors and biochemical characterization of cordon dieback. *Biochem. Cell Biol.* **2008**, *98*, 222–229.
- Trocchi, L.; Calamassi, R.; Mori, B.; Mugnai, L.; Surico, G. *Phaeoconiella chlamydospora*-grapevine interaction: Histochemical reactions to fungal infection. *Phytopathol. Mediterr.* **2001**, *40*, S400–S406.
- Amalfitano, C.; Evidente, A.; Surico, G.; Tegli, S.; Bertelli, E.; Mugnai, L. Phenols and stilbene polyphenols in the wood of esca-diseased grapevines. *Phytopathol. Mediterr.* **2000**, *39*, 178–183.
- Amalfitano, C.; Agrelli, D.; Evidente, A.; Mugnai, L.; Surico, G. Accumulation of viniferins and their reactivity to ROS in the reddish-brown wood of esca diseased grapevine (cv. Sangiovese). 6th International Workshop on Grapevine Trunk Disease, 1–3 September 2008, Florence, Italy.
- Wilson, M. A. *NMR Techniques and Applications in Geochemistry and Soil Chemistry*; Pergamon Press: Oxford, England, 1987; p 353.
- Atalla, R. H.; VanderHart, D. L. The role of solid state ¹³C NMR spectroscopy in studies of the nature of native celluloses. *Solid State Nucl. Magn. Reson.* **1999**, *15*, 1–19.
- Abe, F.; Yamauchi, T. 9 α -hydroxypinoresinol, 9 α -hydroxymedioresinol and related lignans from *Allamanda nerifolia*. *Phytochemistry* **1988**, *27*, 575–577.
- Ralph, S.; Landucci, L.; Ralph, J. *NMR Database of Lignin and Cell Wall Model Compounds*; <http://www.dfrc.ars.usda.gov> (accessed June 12, 2009), in the section 'Products and Services' database, 2004.
- Hannam, K. D.; Quideau, S. A.; Oh, S. W.; Kishchuk, B. E.; Wasylishen, R. E. Forest floor composition in aspen- and spruce-dominated stand of the boreal mixedwood forest. *Soil Sci. Soc. Am. J.* **2004**, *68*, 1735–1743.
- Maunu, S.; Litia, T.; Kauliomaki, S.; Hortling, B.; Sundquist, J. ¹³C CP-MAS NMR investigations of cellulose polymorphs in different pulps. *Cellulose* **2000**, *7*, 147–159.
- Cichewicz, R. H.; Kouzi, S. A. Resveratrol oligomers: Structure, chemistry, and biological activity. In *Studies in Natural Products Chemistry*; Atta-ur-Rahman, Ed.; Elsevier Science B.V.: Amsterdam, Holland, 2002; Vol. 26, pp 507–579.
- Rioux, D.; Nicole, M.; Simard, M.; Ouellette, G. B. Immunocytochemical evidence that secretion of pectin occurs during gel (gum) and tylosis formation in trees. *Phytopathology* **1998**, *88*, 494–505.
- Edwards, J.; Pascoe, I. G.; Salib, S. Impairment of grapevine xylem function by *Phaeoconiella chlamydospora* infection is due to more than physical blockage of vessels with "goo". *Phytopathol. Mediterr.* **2007**, *46*, 87–90.
- Salisbury, F. B.; Riss, C. W. *Fisiologia Vegetale*; Zanichelli: Bologna, Italy, 1994; p 750.
- Rao, C. N. R. *Chemical Applications of Infrared Spectroscopy*; Academic Press: New York, 1963; p 681.
- Gol'man, L. P.; Reznikov, V. M. In *Absorption of Methoxy Groups in the Infrared Spectra of Lignin*; Ispol'z, L., Khim, S. V. M., Eds.; Zinatne: Riga, USSR, 1974; pp 140–148.
- Ishii, T. Structure and function of feruloylated polysaccharides. *Plant Sci.* **1997**, *127*, 111–127.
- Kirk, T. K.; Cowling, E. B. Biological decomposition of solid wood. In *The Chemistry of Solid Wood*; Rowell, R. M., Ed.; Adv. Chem. Ser. 207; American Chemical Society: Washington, DC, 1984; p 614.
- Martinez, A. T.; Almendros, G.; González-Vila, F. J.; Fründ, R. Solid-state spectroscopic analysis of lignins from several Austral hardwoods. *Solid State Nucl. Magn. Reson.* **1999**, *15*, 41–48.
- Bezhuashvili, M. G.; Mudzhiri, L. A.; Zakis, G. F. Structural units of the grapevine lignin. *Koksnes Kimija* **1993**, *4*, 61–63.
- Kirk, T. K.; Higuchi, T.; Chang, H. *Lignin Biodegradation: Microbiology, Chemistry and Potential Applications*; CRC Press: Boca Raton, FL, 1980; Vol. 1, p 241; Vol. 2, p 255.
- Hammel, K. E.; Kapich, A. N.; Jensen, K. A., Jr.; Ryan, Z. C. Reactive oxygen species as agent of wood decay by fungi. *Enzyme Microb. Technol.* **2002**, *30*, 445–453.
- Kerem, Z.; Bao, W.; Hammel, K. E. Rapid polyether cleavage via extracellular one-electron oxidation by a brown-rot basidiomycete. *Proc. Natl. Acad. Sci.* **1998**, *95*, 10373–10377.
- Mittler, R. Oxidative stress, antioxidants and stress tolerance. *Trends Plant Sci.* **2002**, *7*, 405–410.

Received for review June 23, 2009. Revised manuscript received October 22, 2009. Accepted October 23, 2009. Contribution DISSPAPA 201. This study was commissioned by ARSIA-Toscana (Regional Agency for Development and Innovation in Agriculture and Forestry) on behalf of 14 administrative regions and one autonomous province and was funded by Ministero per le Politiche Agricole e Forestali (Ministry of Agriculture and Forestry Policy) to implement the Interregional Project "Esca of Grapevine Research and Experiment in the Nursery and in the Field for Prevention and Cure".